Time-resolved spectroscopy of light emission from plasma generated by a converging strong shock wave in water

D. Yanuka, A. Rososhek, S. Efimov, M. Nitishinskiy, and Ya. E. Krasik
Physics Department, Technion, Haifa 32000, Israel

The results of time-resolved spectroscopic measurements of light emission from plasma formed in the vicinity of a converging spherical strong shock wave (SSW) are reported. This approach, together with hydrodynamic (HD) and radiative-transfer simulations, can be used for the characterization of the SSW convergence symmetry and the parameters of water at that location. It was shown that the obtained time-of-flight of the SSW and emission spectra agree well with the results of the simulation, showing that the water density, temperature, and pressure should be larger than ~ 3 g/cm^{-3}, ~ 1.4 eV, and $\sim 2 \times 10^{11}$ Pa, respectively, at radii $< 25\,\mu$m with respect to the origin of the SSW implosion. *Published by AIP Publishing.* [http://dx.doi.org/10.1063/1.4972042]

The subject of warm dense matter (WDM)[1–4] has been of continuous interest in recent years because of its importance for basic scientific research (astrophysics, equations of state (EOS), conductivity models) and for different applications (x-ray lasers, relativistic electron beams).[5–7] Some of the methods of obtaining WDM include z-pinch, high power lasers, heavy ion beams, and chemical explosions.[8–11] These methods require large amounts of stored energy ($\geq 10^5$ J), large facilities, expensive systems, and special safety measures. Another approach considers the spherical strong shock waves (SSW) which symmetrical convergence results in the formation of WDM in the vicinity of implosion. In earlier studies, these types of SSWs were generated in gas by a reflection of a blast wave from a spherical surface.[12,13] In recent studies,[14] a specially designed gas shock tube allowing a smooth transformation of the initially planar shock wave into a spherical converging SSW was used. This research showed that a non-ideal gas effect governs the parameters of the compressed and ionized gas in the vicinity of implosion.

The results of our recent studies[15,16] indicate that WDM, with a pressure of ~ 2 TPa and temperature of ~ 10 eV, can be obtained using converging SSWs, generated by underwater electrical explosions of quasi-spherical wire arrays (radius ≤ 15 mm), at a distance $\leq 6\,\mu$m from the origin of implosion. These studies were conducted using pulsed power generators with stored energy ≤ 6 kJ and amplitude of the discharge current of ~ 250 kA (rise time of $\sim 1.1\,\mu$s) and ~ 500 kA (rise time of ~ 450 ns). Different indirect methods were applied to determine these water parameters. The time-of-flight (TOF) of the SSW to the origin of the implosion leading to intense light emission from this location was used for comparison with the results of 1D hydrodynamic (HD) simulations,[16] coupled with the equations of state (EOS) of water and copper (the wire's material). In these simulations, which considered a symmetrical SSW convergence, only the energy deposition rate into the wires, calculated using experimentally obtained resistive voltage and discharge current waveforms, was an input parameter. The SSW convergence symmetry was studied using the damage of different targets[17,18] and the change in the parameters of the plasma

preliminarily formed inside a capillary placed in the equatorial plane of the sphere.[19] The data obtained showed that the SSW retains its symmetry along the major part of its convergence ($r < 1$ mm). However, no direct measurement of the water parameters in the vicinity of the implosion ($r < 1$ mm), where the main water compression and heating occurs, was performed.

In this paper, we present the results of direct measurements of the compressed water parameters, i.e., time-resolved spectroscopy of the light emission from the water in the vicinity of the SSW's implosion. These results were then compared with HD and radiative-transfer simulations.

The experiment was carried out using a pulsed power generator with stored energy of ~ 3.6 kJ, rise time of $\sim 1.1\,\mu$s, and peak current of ~ 300 kA for a short circuit load having an inductance similar to the inductance of the spherical wire array (~ 15 nH).[20] The current pulse was applied to a spherical copper wire array, placed inside a stainless steel chamber filled with deionized water. Forty Cu wires $100\,\mu$m in diameter were used for the array, the diameter of which was 30 mm (see Fig. 1). A white plastic ball, shown in Fig. 1, was used to support the wires in the array construction process, and was dissolved using acetone prior to placing the array in the chamber. The number and diameter of the wires were chosen to obtain an overdamped discharge, where most of the stored energy in the generator is delivered to the exploding wires
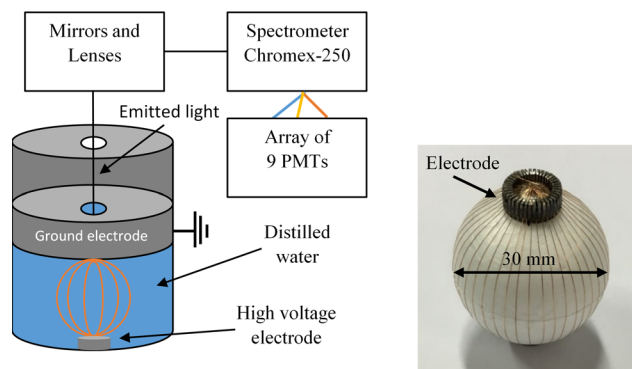
FIG. 1. Experimental setup (left) and spherical wire array before the inner plastic ball (right) was dissolved in acetone.

within a time smaller than half of the period of a periodic discharge. The discharge current and voltage were measured by a self-integrated Rogowski coil and a Tektronix voltage divider, which was connected between the high-voltage and grounded electrodes of the wire array. These electrodes (see Fig. 1) have a hole allowing one to observe the light emitted from the plasma formed by the SSW in the origin's vicinity. This emitted light is passed through an additional collimator placed at the output of the chamber, thus allowing one to obtain the emission from a water volume having a diameter ~2.5 mm, the origin of which is in the center of the sphere. Using mirrors and lenses, the light was focused at the input of an imaging spectrometer (Chromex-250, 0.25 m focal length, 1800 grooves/mm grating). A time-resolved spectrum of this light emission was obtained at the spectrometer's output (see Fig. 1) using a lens and a linear bundle array of optical fibers coupled with an array of 9 Hamamatsu H10721 photomultiplier tubes (PMTs). The relative sensitivity of each PMT was calibrated prior to each shot of the generator to account for its spectral sensitivity.

The spectral resolution (~11 nm/fiber) of this optical system allows a spectral range of ~100 nm for each shot to be observed. Therefore, three ranges of the spectra were studied in different generator shots: 400–500 nm, 500–600 nm, and 580–680 nm. For each range of the spectrum, at least three shots were performed. Typical waveforms of the discharge current $I(t)$ and resistive voltage $\varphi_R = \varphi - L(dI/dt)$ (see Fig. 2(a)) showed an aperiodic type of the discharge characterized by the formation of a low resistive plasma channel (~2 Ω each channel) as a result of the wires' electrical explosion. The light intensities obtained by different PMTs together with the deposited power $P(t) = I(t)\varphi_R(t)$ are shown in Fig. 2(b). One can observe a strong ~1 μs duration light emission starting with a fast increase in the deposited power (main phase of the wire explosion related to the formation of plasma). This emission from the exploding wires was obtained in spite of the collimators, because of the light scattering inside the sphere. At time $\tau \approx 3.7$ μs, one obtains a second light emission. At present, we can consider only that this emission appears as a result of the overlapping of individual SSWs generated by each wire electrical explosion at the line of sight of the pole, to form a single SSW. Finally, one obtains a third strong light emission at $\tau \approx 7.3$ μs with a duration of ~300 ns resulting in the SSW's convergence to the origin. The average time of this third light emission across 9 generator shots was $\tau = 7.2 \pm 0.15$ μs.

Using averaging along 40 ns, time resolved spectra of this emission pulse were obtained. The purpose of this averaging was to decrease the statistical error caused by an insufficient photon flux. A typical spectrum obtained at the peak (±20 ns) of this third light emission is shown in Fig. 3(a). One can see that this spectrum does not contain spectral lines. The latter confirms the results of our earlier measurements performed with a better spectral resolution of ~3 Å/PMT and showing the absence of H_α, H_β and most strong O I and O II spectral lines that indicate the formation of a dense ($>10^{18}$ cm^{-3}) plasma. Therefore, the obtained continuous spectrum can be fitted by the Planckian distribution of a black body (BB) radiation with a temperature of ~0.9 ± 0.12 eV, as a rough estimate. The same BB fit was applied for the spectra obtained around the third emission's peak (±100 ns) in time steps of 20 ns (see Fig. 3(b)). One can see that the BB temperature follows the light intensity and changes in the range 0.6–0.9 eV. Qualitatively similar dependencies of light intensity versus wavelength were obtained in the other generator shots for different ranges of the spectrum. However, because of the shot-to-shot non-reproducibility in the light intensity, it was intolerable to plot a reliable spectrum in the 400–680 wavelength range. Therefore, only the spectra acquired in one shot of the generator was analyzed.

The obtained time-resolved spectra of the intense and short duration light emission acquired at $\tau \approx 7.2 \pm 0.15$ μs from the volume limited by a 2.5 mm diameter can also be used to reconstruct the radial distribution of the density and temperature in the vicinity of the SSW's convergence. The absence of spectral lines and the existence of a continuous spectrum resulting from free-free and free-bound transitions indicate an opaque plasma formed by the SSW's convergence. Thus, one can propose a certain distribution of density and temperature to solve the radiation transfer equation and fit the calculated to the experimentally obtained spectrum. In general, this approach is valid in the case of local thermodynamic equilibrium (LTE), which will be addressed below. The radiative transfer equation considers a beam of light with some frequency ν propagating through a cylinder within a solid angle $\vec{\Omega}$ (Ref. 21)

$$\frac{1}{c}\frac{\partial I_\nu}{\partial t} + \vec{\Omega} \cdot \nabla I_\nu = \kappa_\nu \left(1 - e^{-\frac{h\nu}{kT}}\right)(I_{\nu p} - I_\nu), \quad (1)$$

where c is the speed of light, $I_\nu \left[\frac{W}{sr \cdot m^2}\right]$ is the intensity of the beam, $I_{\nu p}$ is the intensity according to Planck's distribution, k, h, and T are the Boltzmann's constant, Planck's constant,
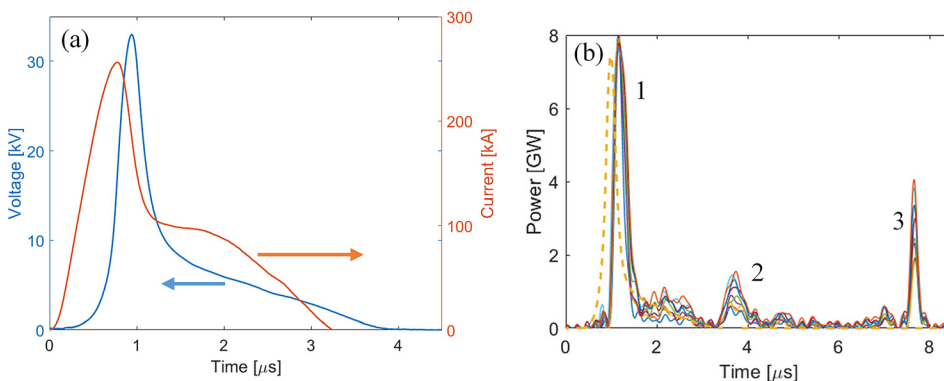
FIG. 2. (a) Waveforms of the discharge current and resistive voltage. (b) Calculated deposited power (dashed line) and recorded intensities from PMTs in arbitrary units. The numbers represent the 3 emissions discussed above.
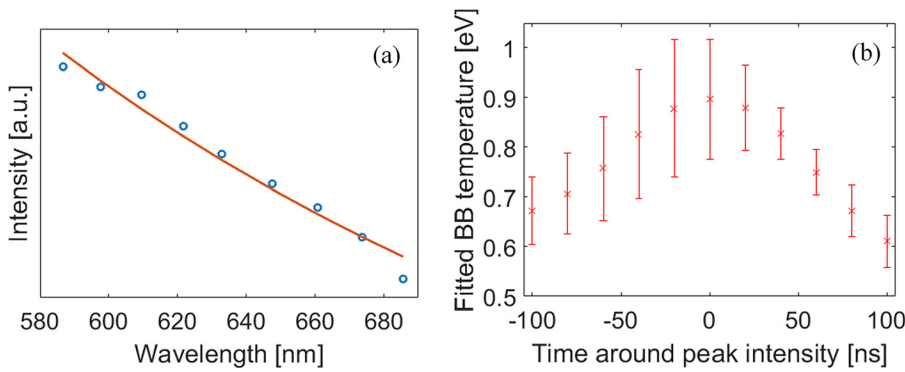
FIG. 3. (a) Typical recorded spectrum at the peak of the third emission with a BB fit showing $T \sim 0.9$ eV. (b) Results of BB fit of the radiation spectra obtained ± 100 ns around the peak intensity of the third emission in time steps of 20 ns and averaged along ± 20 ns.

and the temperature, respectively, and κ_ν is the frequency-dependent absorption coefficient. The steady-state solution of this equation without external sources of radiation is given by

$$I_\nu(s) = \int_{s_0}^{s} \kappa_\nu \left(1 - e^{-\frac{h\nu}{kT}}\right) I_{\nu p} \exp\left[-\int_{s'}^{s} \kappa'_\nu ds''\right] ds', \quad (2)$$

where s is the coordinate along the direction of the beam's propagation. For the considered experimental conditions, s_0 is the center of the sphere, and s is the location of the sphere's grounded electrode through which the light is emitted. In the simulations, the space step along s was $\sim 0.5\,\mu m$.

The proposed radial distributions of the density and temperature are necessary for the calculation of the absorption coefficient $\kappa_\nu(N, T)$ and the intensity according to Planck's distribution $I_{\nu p}(T)$, where N is the number density of the total number of atoms. These distributions were obtained using the results of a 1D HD simulation coupled with the EOS of water and copper.[16] Typical radial distributions of the temperature and density when the SSW approaches $r = 20\,\mu m$ are shown in Fig. 4. The only input to this simulation is the energy deposition rate into the wires, which was calculated using the measured discharge current and resistive voltage waveforms. In addition, this simulation considers a uniform SSW implosion. The TOF of the SSW obtained from this simulation agrees well with the average time of the third light emission pulse's appearance. Applying these distributions, the absorption coefficient for free-free and free-bound transitions was calculated[21]
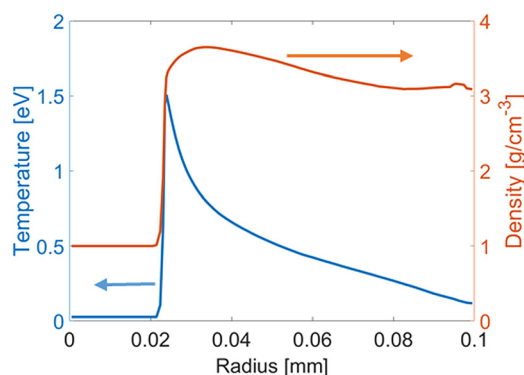
$$\kappa_\nu = \frac{64\pi^4}{3\sqrt{3}} \frac{e^{10} mN}{h^6 c \nu^3} \left[\sum_{n^*}^{\infty} \frac{1}{n^3} e^{-(x_1 - x_n)} + \frac{e^{-x_1}}{2x_1}\right],$$

$$x_1 = \frac{I}{kT}, \quad x_n = \frac{x_1}{n^2}, \quad (3)$$

where e and m are the electron charge and mass, respectively, I is the ionization energy of the hydrogen atom from the ground level, and n^* is the energy level for which $h\nu \geq E_{n^*}$, where E_{n^*} is the ionization energy from level n^*. This summation can be cut off by the effective quantum number above which the energy levels can be considered to be continuous. This effective quantum number was calculated using Inglis-Teller's formula[22] $n_{max} \approx 10^3 \times n_p^{-2/15}$ considering the energy level overlapping due to Stark broadening, where n_p is the density of plasma electrons calculated using the Saha equation.[21]

To verify that the radiation is in LTE, the mean-free-path of a photon $l_\nu = 1/\kappa_\nu$ should be smaller than the distance for which the change in the temperature becomes significant, i.e., by an order of magnitude or more (in our case the change in temperature is $\sim 40\%$). Calculations showed $l_\nu \sim 10\,\mu m$ for $\lambda = 400$ nm, for which the value of l_ν is the longest in the spectrum obtained. The value of l_ν is smaller than the thickness of the spherical layer of $\sim 30\,\mu m$, which, as shown below, makes the main contribution to the intensity of the light. In addition, a steady state condition is valid if the time scale of the light emission pulse is much larger than the time it takes a photon to travel this distance. The latter is $\tau = l_\nu/c \sim 10^{-14}$ s, which is much smaller than the duration of the considered light emission.

The results of these radiative transfer simulations showed that, as the SSW propagates toward the origin, the spectrum of the light emission is changing very fast, as shown in Fig. 5. Namely, if at $r \sim 120\,\mu m$ the slope of the spectrum is positive, at $r \sim 20\,\mu m$, this slope becomes negative. This is explained by the drastic change in the radial distribution of temperature shown in Fig. 5(b). Let us note here that for the distributions shown in Fig. 5, the SSW TOF between radii $\sim 120\,\mu m$ and $\sim 20\,\mu m$ is 8.5 ns, resulting in an average Mach velocity of 8. Further, the results of simulations showed that at $r < 25\,\mu m$, the negative slope of the spectrum does not change significantly despite the fact that the SSW continues to propagate toward the origin. This negative slope of the emission spectrum is similar to the recorded spectrum (see Fig. 3). Thus, one can consider the SSW uniform convergence until $r = 25\,\mu m$ (compression

FIG. 4. Calculated distributions of temperature and density when SSW arrives to $\sim 20\,\mu m$ radius.
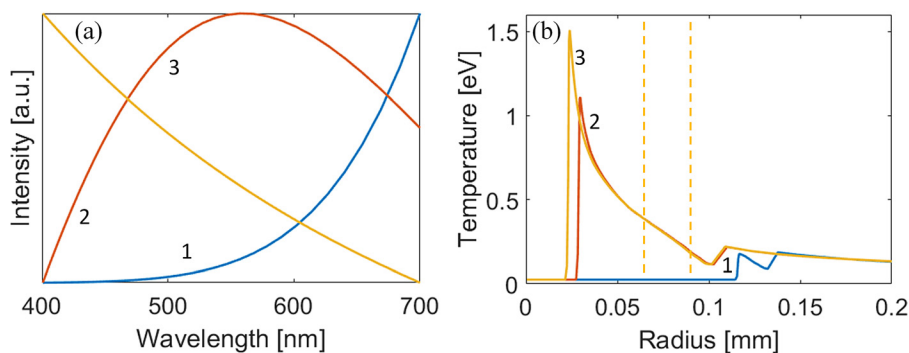
FIG. 5. Calculated distribution of (a) emitted light intensity and (b) temperature for three different times. The numbers near the curves in (a) correspond to those in (b). The duration of the process is ~8.5 ns. The two dashed lines in (b) show the part which contributes to the emitted spectrum for curve 3.
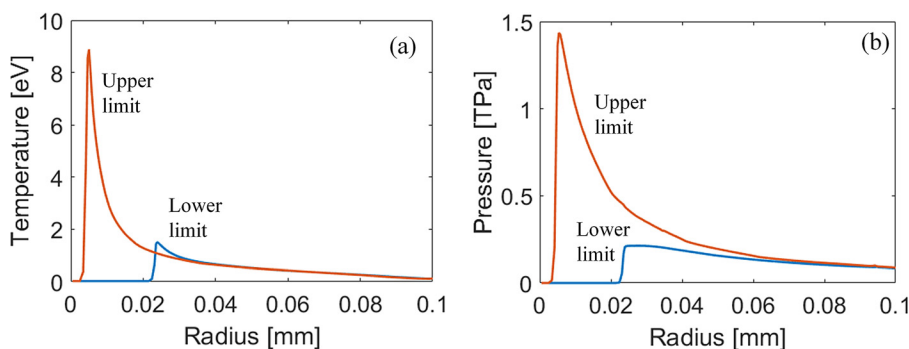
FIG. 6. Lower and upper limit in radial distributions of (a) temperature and (b) pressure in the vicinity of implosion.

factor of 600) and use this as a lower limit for the water parameters' distributions shown in Fig. 6. Let us note that the time jitter of ~150 μs in the TOF of the SSW results in a change in these calculated water parameters of <10%.

For the case of the upper limit of the water parameters, i.e., uniform SSW convergence at $r < 25\,\mu$m, one can consider the results of the HD simulations corresponding to the distribution shown in Fig. 6, where the SSW approaches $r = 5\,\mu$m.

To conclude, time-resolved spectroscopic measurements of the light emission from the plasma formed in the vicinity of the converging SSW implosion showed that this approach together with HD and radiative-transfer simulations can be used for estimation of the SSW convergence symmetry and the parameters of water at that location. It was shown that the SSW TOF obtained and the emission spectra agree well with the results of the simulation showing that the water density, temperature, and pressure should be greater than ~3 g/cm^{-3}, ~1.4 eV, and ~2 × 10^{11} Pa. Using a smaller diameter quasi-spherical wire array made of Al wires and a larger energy stored in the pulse generator, one can expect to obtain much larger parameters of water in larger volumes in the vicinity of the SSW's implosion. We are planning to perform these experiments.

[1]S. H. Glenzer, O. L. Landen, P. Neumayer, R. W. Lee, K. Widmann, S. W. Pollaine, and R. J. Wallace, Phys. Rev. Lett. **98**, 065002 (2007).
[2]R. Ernstorfer, M. Harb, C. T. Hebeisen, G. Sciaini, T. Dartigalongue, and R. J. Dwayne Miller, Science **323**, 1033 (2009).
[3]M. Koenig, A. Benuzzi-Mounaix, A. Ravasio, T. Vinci, N. Ozaki, S. Lepape, D. Batani, G. Huser, T. Hall, D. Hicks, A. MacKinnon, P. Patel, H. S. Park, T. Boehly, M. Borghesi, S. Kar, and L. Romagnani, Plasma Phys. Controlled Fusion **47**, B441 (2005).
[4]V. E. Fortov and I. T. Iakubov, *The Physics of Non-Ideal Plasma* (World Scientific, Singapore, 2000).
[5]J. J. Rocca, V. Shlyaptsev, F. G. Tomasel, O. D. Cortazar, D. Hartshorn, and J. L. A. Chilla, Phys. Rev. Lett. **73**, 2192 (1994).
[6]R. P. Drake, Phys. Plasmas **16**, 055501 (2009).
[7]V. A. Burtsev, N. V. Kalinin, and A. V. Luchinsky, *Electrical Explosion of Conductors* (Energoatomisdat, Moscow, 1990).
[8]I. M. Hall, T. Durmaz, R. C. Mancini, J. E. Bailey, G. A. Rochau, I. E. Golovkin, and J. J. MacFarlane, Phys. Plasmas **21**, 031203 (2014).
[9]B. A. Remington, R. P. Drake, and D. D. Ryutov, Rev. Mod. Phys. **78**, 755 (2006).
[10]N. A. Tahir, D. H. H. Hoffmann, A. Kozyreva, A. Shutov, J. A. Maruhn, U. Neuner, A. Tauschwitz, P. Spiller, and R. Bock, Phys. Rev. E **61**, 1975 (2000).
[11]E. N. Avrorin, B. K. Vodolaga, V. A. Simonenko, and V. E. Fortov, Phys.-Usp. **36**(5), 337–364 (1993).
[12]T. Saito and I. I. Glass, Proc. R. Soc. London A **384**, 217–231 (1982).
[13]S. H. R. Hosseini and K. Takayama, Shock Waves **20**, 1–7 (2010).
[14]M. Liverts and N. Apazidis, Phys. Rev. Lett. **116**, 014501 (2016).
[15]O. Antonov, S. Efimov, D. Yanuka, M. Kozlov, V. Tz. Gurovich, and Ya. E. Krasik, Appl. Phys. Lett. **102**, 124104 (2013).
[16]O. Antonov, L. Gilburd, S. Efimov, G. Bazalitski, V. Tz. Gurovich, and Ya. E. Krasik, Phys. Plasmas **19**, 102702 (2012).
[17]O. Antonov, S. Efimov, V. Tz. Gurovich, D. Yanuka, D. Shafer, and Ya. E. Krasik, J. Appl. Phys. **115**, 223303 (2014).
[18]O. Antonov, S. Efimov, V. Tz. Gurovich, V. Bernshtam, and Ya. E. Krasik, Phys. Plasmas **22**, 053507 (2015).
[19]M. Nitishinskiy, S. Efimov, O. Antonov, D. Yanuka, V. Tz. Gurovich, V. Bernshtam, V. Fisher, and Ya. E. Krasik, Phys. Plasmas **23**, 042705 (2016).
[20]S. Efimov, A. Fedotov, S. Gleizer, V. Tz. Gurovich, G. Bazalitski, and Ya. E. Krasik, Phys. Plasmas **15**, 112703 (2008).
[21]Ya. B. Zeldovich and Yu. P. Raizer, *Physics of Shock Waves and High-Temperature Hydrodynamic Phenomena* (Academic Press, New York/London, 1966).
[22]D. R. Inglis and E. Teller, ApJ. **90**, 439 (1939).